

## Global Status of Sterile Neutrino Scenarios

---

**Joachim KOPP\***

*Max Planck Institut für Kernphysik, Heidelberg*

*E-mail: [jkopp@mpi-hd.mpg.de](mailto:jkopp@mpi-hd.mpg.de)*

**Pedro A. N. MACHADO**

*Instituto de Física, Universidade de São Paulo and*

*Departamento de Física Teórica and Instituto de Física Teórica, UAM/CSIC, Madrid*

*E-mail: [pedro.machado@uam.es](mailto:pedro.machado@uam.es)*

**Michele MALTONI**

*Instituto de Física Teórica, UAM/CSIC, Madrid*

*E-mail: [michele.maltoni@csic.es](mailto:michele.maltoni@csic.es)*

**Thomas SCHWETZ**

*Max Planck Institut für Kernphysik, Heidelberg*

*E-mail: [schwetz@mpi-hd.mpg.de](mailto:schwetz@mpi-hd.mpg.de)*

We discuss the current status of neutrino oscillations in models with more than three light neutrino flavors. In particular, we present results of a global fit to short and long baseline oscillation data from reactor, accelerator, atmospheric, solar, and radioactive source experiments. We examine to what extent experimental hints for oscillations involving sterile neutrinos—in particular the reactor and gallium anomalies as well as the MiniBooNE and LSND results—are compatible with null results from other experiments. In all cases, we find severe tension in the global fit, which leads us to the conclusion that models augmenting the Standard Model only by one or several eV-scale sterile neutrinos are unable to explain all short-baseline anomalies simultaneously.

*XV International Workshop on Neutrino Telescopes*

*March 11-15 2013*

*Venice, Italy*

---

\*Speaker.

## 1. Introduction

In recent years, models with more than three light neutrino flavors have received a tremendous amount of attention, mostly because of several intriguing experimental anomalies that could be explained in such models. Specifically, the long-standing excess of  $\bar{\nu}_e$  events from a  $\bar{\nu}_\mu$  source in the short baseline (SBL) experiment LSND [1] could be understood if both  $\bar{\nu}_e$  and  $\bar{\nu}_\mu$  contain a small admixture of a hypothetical  $\mathcal{O}(\text{eV})$  neutrino mass eigenstate. In the same way, also the more recent MiniBooNE anomaly [2, 3]—an excess of  $\bar{\nu}_e$  events in a  $\bar{\nu}_\mu$  beam—could be explained. Finally, there are hints for anomalous  $\nu_e$  and  $\bar{\nu}_e$  disappearance at very short baselines from reactor experiments [4–7] and from experiments using intense radioactive sources [8, 9]. These signals could also be understood if electron neutrinos oscillate into sterile flavors.

On the other hand, a large number of experiments that did not observe any anomalies put severe constraints on the parameter space of sterile neutrino models [10–16]. In this talk, which is based on reference [15] we quantify the tension between the anomalies and the null results by carrying out a global fit to the data. Our fits were obtained in a GLOBES-based framework [17, 18], together with fitting codes from [15, 19–24]. Details on the employed methodology, as well as further references, are given in [15].

We augment the Standard Model with one or two additional neutrino states with masses around 1 eV, and with small mixing with the three conventional neutrino mass eigenstates  $\ll 1$  eV. We call the scenario with one extra neutrino species a 3+1 model, and the scenario with two new states a 3+2 model. In addition, we also consider a “1+3+1” model, where one of the mostly sterile states is almost massless, the three mostly active states are at around 1 eV, and the second mostly sterile state is even heavier. We remark, though, that it is very difficult to reconcile such a model with cosmological constraints. The most important difference between the model with one new neutrino mass eigenstate and models with two new mass eigenstates is the possibility of CP violation already at short baseline in the latter case. We denote the mass squared differences between the three mostly active mass eigenstates  $\nu_1, \nu_2, \nu_3$  and the mostly sterile states  $\nu_4, \nu_5$  by  $\Delta m_{ij}^2 \equiv m_i^2 - m_j^2$  for  $i, j = 1 \dots 5$ . The unitary mixing matrix has the elements  $U_{\alpha i}$  with  $i = 1 \dots 5$  and  $\alpha = e, \mu, \tau$  for the active flavor eigenstates and  $\alpha = s_1, s_2$  for the sterile ones. We parameterize  $U$  as

$$U = V_{35} O_{34} V_{25} V_{24} O_{23} O_{15} O_{14} V_{13} V_{12}, \quad (1.1)$$

where we denote a real rotation matrix in the  $(ij)$ -plane by  $O_{ij}$ , and a complex rotation matrix by  $V_{ij}$ . The corresponding mixing angle is  $\theta_{ij}$ , and the phase in  $V_{ij}$  is denoted by  $\varphi_{ij}$ .

## 2. $\nu_e$ and $\bar{\nu}_e$ disappearance

We begin by analyzing electron (anti)neutrino disappearance experiments alone. In the 3+1 model, the  $\bar{\nu}_e$  survival probability at short baseline [ $\Delta m_{31}^2 L/2E \ll 1, \Delta m_{21}^2 L/2E \ll 1$ ], is given by

$$P_{ee}^{\text{SBL},3+1} = 1 - 4|U_{e4}|^2(1 - |U_{e4}|^2) \sin^2 \frac{\Delta m_{41}^2 L}{4E} \equiv 1 - \sin^2 2\theta_{ee} \sin^2 \frac{\Delta m_{41}^2 L}{4E}, \quad (2.1)$$

where we have implicitly defined the effective 2-flavor mixing angle  $\theta_{ee}$ . The results of our numerical fit for  $\nu_e$  and  $\bar{\nu}_e$  disappearance are shown in figure 1. We see that this subset of the global

Experiment	ref.	dof	channel	comments
Short-baseline (SBL) reactors	76	$\bar{\nu}_e \rightarrow \bar{\nu}_e$	SBL	
Long-baseline (LBL) reactors	39	$\bar{\nu}_e \rightarrow \bar{\nu}_e$	LBL	
KamLAND	17	$\bar{\nu}_e \rightarrow \bar{\nu}_e$		
Gallium	4	$\nu_e \rightarrow \nu_e$	SBL	
Solar neutrinos	261	$\nu_e \rightarrow \nu_e + \text{NC data}$		
LSND/KARMEN $^{12}\text{C}$	32	$\nu_e \rightarrow \nu_e$	SBL	
CDHS	15	$\nu_\mu \rightarrow \nu_\mu$	SBL	
MiniBooNE $\nu$	15	$\nu_\mu \rightarrow \nu_\mu$	SBL	
MiniBooNE $\bar{\nu}$	42	$\bar{\nu}_\mu \rightarrow \bar{\nu}_\mu$	SBL	
MINOS CC	20	$\nu_\mu \rightarrow \nu_\mu$	LBL	
MINOS NC	20	$\nu_\mu \rightarrow \nu_s$	LBL	
Atmospheric neutrinos	80	$\overset{(-)}{\nu}_\mu \rightarrow \overset{(-)}{\nu}_\mu + \text{NC matter effect}$		
LSND	11	$\bar{\nu}_\mu \rightarrow \bar{\nu}_e$	SBL	
KARMEN	9	$\bar{\nu}_\mu \rightarrow \bar{\nu}_e$	SBL	
NOMAD	1	$\nu_\mu \rightarrow \nu_e$	SBL	
MiniBooNE $\nu$	11	$\nu_\mu \rightarrow \nu_e$	SBL	
MiniBooNE $\bar{\nu}$	11	$\bar{\nu}_\mu \rightarrow \bar{\nu}_e$	SBL	
E776	24	$\overset{(-)}{\nu}_\mu \rightarrow \overset{(-)}{\nu}_e$	SBL	
ICARUS	1	$\nu_\mu \rightarrow \nu_e$	LBL	
total	689			

**Table 1:** Summary of the data used in this work divided into  $\overset{(-)}{\nu}_e$ ,  $\overset{(-)}{\nu}_\mu$  disappearance, and appearance data. The column “dof” gives the number of data points used in our analysis minus the number of free nuisance parameters for each experiment. Table taken from [15], where also more details on the analysis and a complete list of references to the relevant experimental papers are given.

	$\sin^2 2\theta_{14}$	$\Delta m_{41}^2 [\text{eV}^2]$	$\chi_{\text{min}}^2/\text{dof}$ (GOF)	$\Delta\chi_{\text{no-osc}}^2/\text{dof}$ (CL)
SBL	0.10	1.75	58.3/74 (91%)	9.0/2 (98.9%)
SBL + Gallium	0.11	1.80	64.0/78 (87%)	14.0/2 (99.9%)
SBL + LBL	0.09	1.78	93.0/113 (92%)	9.2/2 (99.0%)
global $\nu_e$ disapp.	0.09	1.78	403.3/427 (79%)	12.6/2 (99.8%)

**Table 2:** Results of our global fit to  $\nu_e$  and  $\bar{\nu}_e$  disappearance data. We show the best fit values for the oscillation parameters  $\sin^2 \theta_{14}$  and  $\Delta m_{41}^2$ , the minimum  $\chi^2$  values divided by the number of degrees of freedom as a measure of the goodness of fit (GOF), and the  $\Delta\chi^2$  and confidence level at which the no oscillation hypothesis is disfavored. The row “global  $\nu_e$  disapp.” includes the data from short-baseline (SBL) and long baseline (LBL) reactor experiments as well as gallium data, solar neutrinos and the LSND/KARMEN  $\nu_e$  disappearance data from  $\nu_e$ - $^{12}\text{C}$  scattering. In our fits, we have marginalized  $\chi^2$  over the mixing angles  $\theta_{12}$  and  $\theta_{13}$ . Table taken from [15].

data can be consistently interpreted in a 3+1 model This conclusion is confirmed by table 2, which shows that the goodness of fit (measured in terms of the  $\chi^2$  per degree of freedom) remains excellent even when the anomalous short baseline reactor and gallium data are combined with long baseline reactor data, solar+KamLAND data, and with the  $\nu_e$ - $^{12}\text{C}$  scattering data from KARMEN and LSND.

The fit prefers a fourth neutrino state with a mass  $\gtrsim 0.5$  eV, and with order 10% mixing with the electron (anti)neutrino. From the oscillation data alone, the mass of the mostly sterile eigenstate

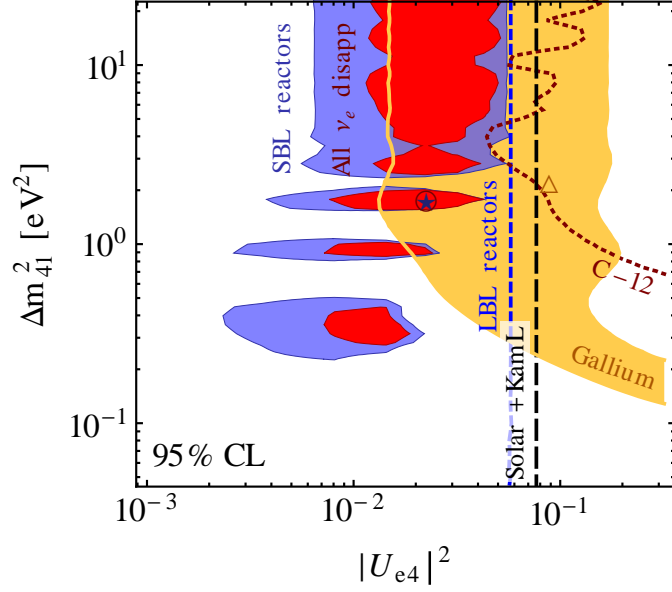


**Figure 1:** Preferred parameter regions and exclusion limits at the 95% confidence level from the fit of a 3+1 model to  $\nu_e$  and  $\bar{\nu}_e$  disappearance data only. We find that the region favored by the reactor anomaly (blue region) and by the gallium anomaly (yellow region) are consistent with the exclusion limits from long-baseline reactor experiments (blue dashed line), from solar + KamLAND data (black long dashed line), and  $\nu_e$ - $^{12}\text{C}$  scattering data from LSND and KARMEN (dark red dotted line). The red shaded region and the open circle show the allowed parameter range and best fit point from the combined analysis of these data sets. In our fits, we have marginalized  $\chi^2$  over the mixing angles  $\theta_{12}$  and  $\theta_{13}$ . Figure taken from [15].

is only very weakly constrained from above because it is only restricted by the fact that it has to be kinematically accessible in the  $\mathcal{O}(\text{MeV})$  neutrino sources considered here. However, direct kinematic neutrino searches disfavor masses above  $\sim \mathcal{O}(100 \text{ eV})$  if the mixing is large enough to explain the reactor and gallium anomalies [25–27].

We have also checked that the possible presence of sterile neutrinos does not affect the measurement of the mixing angle  $\theta_{13}$ . (see also [28, 29]).

### 3. $\nu_e$ and $\bar{\nu}_e$ appearance

We next consider the  $\bar{\nu}_\mu \rightarrow \bar{\nu}_e$  oscillations searches in LSND, MiniBooNE, KARMEN, NOMAD, E776 and ICARUS. The oscillation probability in this channel for the 3+1 scheme at short baseline is given by

$$P_{\bar{\nu}_\mu \rightarrow \bar{\nu}_e}^{\text{SBL},3+1} = 4|U_{\mu 4}U_{e4}|^2 \sin^2 \frac{\Delta m_{41}^2 L}{4E} \equiv \sin^2 2\theta_{\mu e} \sin^2 \frac{\Delta m_{41}^2 L}{4E}, \quad (3.1)$$

where we have again defined an effective 2-flavor mixing angle  $\sin^2 2\theta_{\mu e}$ . As shown in figure 2, this subset of the global oscillation data can be fit consistently as well. In the 3+1 scenario, the best fit point is at  $\sin^2 2\theta_{\mu e} = 0.013$ ,  $\Delta m_{41}^2 = 0.42 \text{ eV}^2$ , and the fit strongly excludes the no oscillation hypothesis with  $\Delta\chi^2 = 47.7$ .

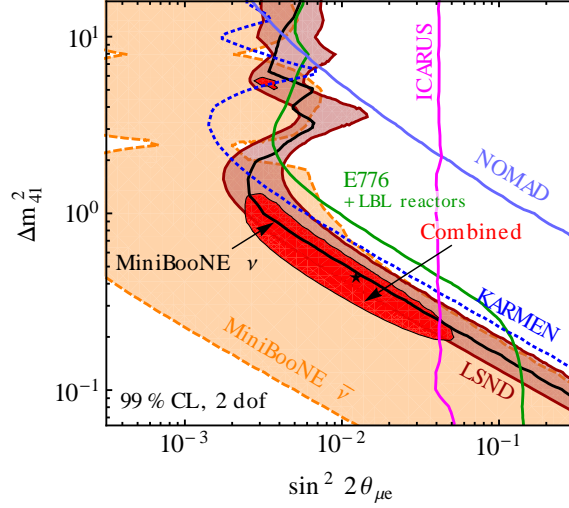


**Figure 2:** Parameter space for  $\bar{\nu}_\mu \rightarrow \bar{\nu}_e$  appearance experiments in the 3+1 framework. We show the exclusion limits from KARMEN (blue dotted), NOMAD (blue solid), ICARUS (pink solid), E776 (green solid) and MiniBooNE neutrino-mode data (black solid), as well as the preferred parameter regions from LSND (shaded dark red), MiniBooNE antineutrino data (shaded orange), and from the global fit to all aforementioned data sets (light red shaded). All results are shown at the 99% CL for 2 degrees of freedom. In the fits, we have marginalized over the relevant complex phases. Note that E776 data in our fit is combined with long baseline reactor data to constrain oscillations of the  $\bar{\nu}_e$  background. We see that  $\bar{\nu}_\mu \rightarrow \bar{\nu}_e$  appearance data alone lead to a consistent fit, with a preference for non-zero admixture of sterile neutrinos. Figure taken from [15].

For two sterile neutrinos, the goodness of fit—which is already good in the 3+1 case—improves substantially, with the largest improvement coming from the MiniBooNE neutrino data. Quantitatively, the  $\chi^2$  per degree of freedom (dof) is 87.9/66 for the 3+1 model and 72.7/63 for the 3+2 model. In the 1+3+1 scenario, we obtain  $\chi^2/\text{dof} = 74.6/63$ .

#### 4. $\nu_\mu, \bar{\nu}_\mu$ and neutral current disappearance searches

We have seen in equations (2.1) and (3.1) that  $\bar{\nu}_e$  disappearance at short baseline is sensitive to the mixing matrix element  $|U_{e4}|$ , while  $\bar{\nu}_e$  appearance searches probe the combination  $|U_{e4}U_{\mu 4}|$ . Thus, an independent measurement of  $U_{\mu 4}$  would over-constrain the 3+1 scenario. Such a measurement is available from experiments searching for  $\bar{\nu}_\mu$  disappearance, the probability for which is at short baseline approximately given by

$$P_{\mu\mu}^{\text{SBL},3+1} = 1 - 4|U_{\mu 4}|^2(1 - |U_{\mu 4}|^2) \sin^2 \frac{\Delta m_{41}^2 L}{4E} \equiv 1 - \sin^2 2\theta_{\mu\mu} \sin^2 \frac{\Delta m_{41}^2 L}{4E}. \quad (4.1)$$

In figure 3 we show exclusion limits from  $\bar{\nu}_\mu$  disappearance searches, together with the parameter region preferred by a combined fit to the anomalous LSND, MiniBooNE, reactor and gallium data. We see that there is severe tension between the short baseline anomalies and the exclusion limit from the null experiments.

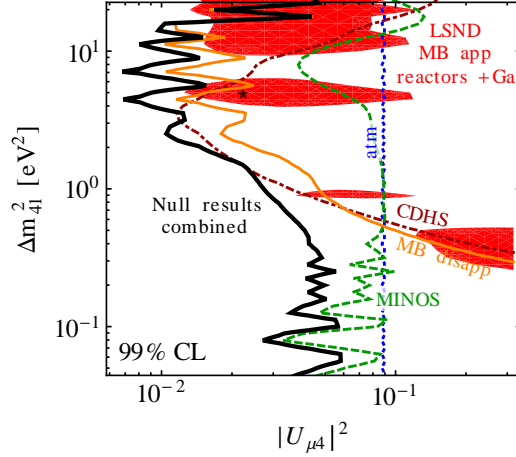


**Figure 3:** Constraints in the  $|U_{\mu 4}|^2 - \Delta m_{41}^2$  plane from  $\bar{\nu}_\mu$  disappearance searches (colored lines), compared to the parameter region preferred by a fit to the anomalous LSND, MiniBooNE, reactor and gallium data (red region). All results are shown at 99% CL (2 dof). In the fit to  $\bar{\nu}_\mu$  disappearance data, we minimize  $\chi^2$  with respect to  $|U_{\tau 4}|$  and the complex phase  $\varphi_{24}$ , while for the  $\bar{\nu}_e$  appearance searches, we marginalize over  $|U_{e 4}|^2$ . Figure taken from [15].

## 5. The global picture

We now combine the above results into a global fit in order to quantify the tension found in section 4. Figure 4 confirms the disagreement between the anomalous short baseline results and the null experiments. To make a more quantitative statement, we have carried out a parameter goodness of fit test [30], which measures by how much the  $\chi^2$  worsens when appearance and disappearance data are fit together. More precisely, we define

$$\chi_{\text{PG}}^2 = (\chi_{\text{app, global}}^2 - \chi_{\text{app, min}}^2) + (\chi_{\text{disapp, global}}^2 - \chi_{\text{disapp, min}}^2), \quad (5.1)$$

where  $\chi_{\text{app, global}}^2$  is the  $\chi^2$  from appearance experiments evaluated at the global best fit point, and  $\chi_{\text{app, min}}^2$  is the  $\chi^2$  from appearance experiments evaluated at the appearance only best fit point.  $\chi_{\text{disapp, global}}^2$  and  $\chi_{\text{disapp, min}}^2$  are defined analogously. We see from table 3 that the probability for the tension between appearance and disappearance data being due to statistical fluctuations is at the  $10^{-4}$  level for the 3+1 model, and even worse for the 3+2 model. The poorer agreement in the 3+2 case is due to the significant improvement in the appearance only fit in this case (see section 3), which is not accompanied by a similar improvement in the global fit. The global best fit points for the 3+1, 3+2 and 1+3+1 models are given in table 4.

## 6. Sterile neutrinos and cosmology

Besides their possible relevance for neutrino oscillation experiments, eV-scale sterile neutrinos would also have profound implications for cosmology. In particular, if thermalized in the early Universe, they would contribute to the total number of relativistic degrees of freedom, often parameterized in terms of the effective number of neutrino species  $N_{\text{eff}}$ . Recent data on  $N_{\text{eff}}$

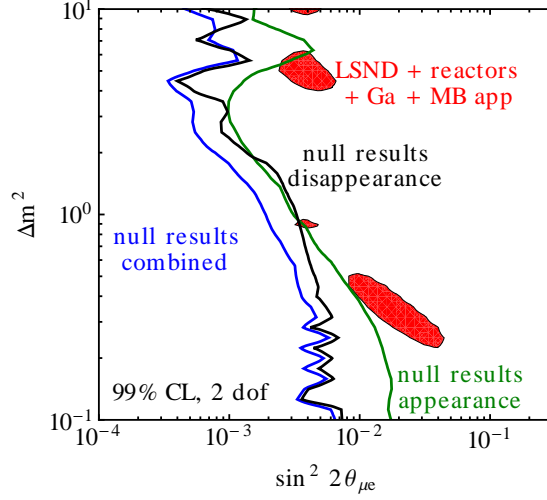


**Figure 4:** Results of the global fit in the 3+1 scenario, shown as exclusion limits and allowed regions for the effective mixing angle  $\sin^2 2\theta_{\mu e} = 4|U_{e4}|^2|U_{\mu 4}|^2$  and the mass squared difference  $\Delta m_{41}^2$ . We compare the regions preferred by experiments reporting possible hints for sterile neutrinos (LSND, MiniBooNE, SBL reactor, gallium) to the exclusion limits from other data (blue). We also show separate exclusion limits from null results in disappearance searches (black) and in appearance searches (green). Figure taken from [15].

	$\chi_{\min}^2/\text{dof}$	GOF	$\chi_{\text{PG}}^2/\text{dof}$	PG	$\chi_{\text{app, glob}}^2$	$\Delta\chi_{\text{app}}^2$	$\chi_{\text{dis, glob}}^2$	$\Delta\chi_{\text{dis}}^2$
3+1	712/(689–9)	19%	18.0/2	$1.2 \times 10^{-4}$	95.8/68	7.9	616/621	10.1
3+2	701/(689–14)	23%	25.8/4	$3.4 \times 10^{-5}$	92.4/68	19.7	609/621	6.1
1+3+1	694/(689–14)	30%	16.8/4	$2.1 \times 10^{-3}$	82.4/68	7.8	611/621	9.0

**Table 3:** Quantitative statistical results for the global fit in the 3+1, 3+2 and 1+3+1 scenarios. We show the global minimum  $\chi^2$  per degree of freedom, the corresponding goodness of fit and the results from a parameter goodness-of-fit (PG) test [30]. In the last four columns we report the contributions of appearance and disappearance data to  $\chi_{\text{PG}}^2$ , see equation (5.1). Table taken from [15].

	$\Delta m_{41}^2$ [eV <sup>2</sup> ]	$ U_{e4} $	$ U_{\mu 4} $	$\Delta m_{51}^2$ [eV <sup>2</sup> ]	$ U_{e5} $	$ U_{\mu 5} $	$\gamma_{\mu e}$
3+1	0.93	0.15	0.17				
3+2	0.47	0.13	0.15	0.87	0.14	0.13	$-0.15\pi$
1+3+1	-0.87	0.15	0.13	0.47	0.13	0.17	$0.06\pi$

**Table 4:** Global best fit points for the 3+1, 3+2, and 1+3+1 models.  $\gamma_{\mu e}$  is the complex phase relevant for SBL appearance experiments, defined as  $\gamma_{\mu e} \equiv \arg(U_{e4}^* U_{\mu 4} U_{e5} U_{\mu 5}^*)$ .

from the Planck satellite mildly disfavors the existence of a fully thermalized light sterile neutrino species [31].

Sterile neutrinos could also affect structure formation by efficiently transporting energy over large distances, thus washing out small scale structure. The relevant parameter, the sum of the masses of all thermalized neutrino states  $\sum m_\nu$ , is constrained to be below about 0.5 eV [31]. (The exact constraint depends on which cosmological data sets are considered.)

Therefore, we see that sterile neutrinos with the mass scale required to mitigate the short baseline anomalies, are in severe conflict with cosmology, provided they are thermalized in the early

Universe. For the  $\mathcal{O}(10\%)$  mixings with active neutrinos preferred by the oscillation data, this is indeed expected, see for instance [32]. Modifications of  $\Lambda$ CDM cosmology that could reconcile thermalized sterile neutrinos with cosmological data have been investigated in [33]. Moreover, it has been shown that in non-minimal sterile neutrino models, thermalization can be avoided altogether, for instance due to a very low reheating temperature [34], due to entropy production in the visible sector after neutrino decoupling [35, 36], or due to dynamic suppression of active–sterile neutrino mixing. Such dynamic suppression could have its origin in a large lepton asymmetry [37–39], in the existence of a Majoron field [40], or in new gauge interactions in the sterile neutrino sector [41, 42].

## 7. Conclusions

In summary, we have shown that it is very difficult to reconcile all short and long baseline neutrino oscillation data within a sterile neutrino framework. The substantial tension we have found between the anomalous results from LSND, MiniBooNE, reactor and gallium experiments, and the null results from many other experiments, suggests that some or all of the anomalies are not due to sterile neutrinos. Alternatively, one should also seriously consider the possibility that some of the exclusion limits are too strong. Finally, an interesting avenue for future research are extended models in which sterile neutrinos have non-trivial dynamics beyond their mixing with active neutrinos [43]. Such non-standard dynamics could also reconcile the existence of sterile neutrinos with cosmology.

## Acknowledgments

It is a pleasure to thank the organizers of the 15th International Workshop on Neutrino Telescopes for a very enjoyable and productive conference, with many inspiring discussions.

- [1] **LSND** Collaboration, A. Aguilar et al., *Evidence for neutrino oscillations from the observation of  $\bar{\nu}_e$  appearance in a  $\bar{\nu}_\mu$  beam*, *Phys. Rev.* **D64** (2001) 112007, [[hep-ex/0104049](#)].
- [2] **MiniBooNE** Collaboration, A. Aguilar-Arevalo et al., *Event Excess in the MiniBooNE Search for  $\bar{\nu}_\mu \rightarrow \bar{\nu}_e$  Oscillations*, *Phys.Rev.Lett.* **105** (2010) 181801, [[arXiv:1007.1150](#)].
- [3] **MiniBooNE Collaboration** Collaboration, A. Aguilar-Arevalo et al., *Improved Search for  $\bar{\nu}_\mu \rightarrow \bar{\nu}_e$  Oscillations in the MiniBooNE Experiment*, *Phys.Rev.Lett.* **110** (2013) 161801, [[arXiv:1207.4809](#)].
- [4] T. Mueller et al., *Improved Predictions of Reactor Antineutrino Spectra*, *Phys.Rev.* **C83** (2011) 054615, [[arXiv:1101.2663](#)].
- [5] G. Mention et al., *The Reactor Antineutrino Anomaly*, *Phys.Rev.* **D83** (2011) 073006, [[arXiv:1101.2755](#)].

- [6] P. Huber, *On the determination of anti-neutrino spectra from nuclear reactors*, *Phys.Rev.* **C84** (2011) 024617, [[arXiv:1106.0687](#)].
- [7] A. Hayes, J. Friar, G. Garvey, and G. Jonkmans, *Reanalysis of the Reactor Neutrino Anomaly*, [arXiv:1309.4146](#).
- [8] M. A. Acero, C. Giunti, and M. Laveder, *Limits on  $\nu(e)$  and anti- $\nu(e)$  disappearance from Gallium and reactor experiments*, *Phys.Rev.* **D78** (2008) 073009, [[arXiv:0711.4222](#)].
- [9] C. Giunti and M. Laveder, *Statistical Significance of the Gallium Anomaly*, *Phys.Rev.* **C83** (2011) 065504, [[arXiv:1006.3244](#)].
- [10] M. Maltoni, T. Schwetz, M. Tortola, and J. Valle, *Ruling out four neutrino oscillation interpretations of the LSND anomaly?*, *Nucl.Phys.* **B643** (2002) 321–338, [[hep-ph/0207157](#)].
- [11] A. Strumia, *Interpreting the LSND anomaly: Sterile neutrinos or CPT violation or...?*, *Phys.Lett.* **B539** (2002) 91–101, [[hep-ph/0201134](#)].
- [12] M. Cirelli, G. Marandella, A. Strumia, and F. Vissani, *Probing oscillations into sterile neutrinos with cosmology, astrophysics and experiments*, *Nucl.Phys.* **B708** (2005) 215–267, [[hep-ph/0403158](#)].
- [13] C. Giunti and M. Laveder, *Status of 3+1 Neutrino Mixing*, *Phys.Rev.* **D84** (2011) 093006, [[arXiv:1109.4033](#)].
- [14] J. Conrad, C. Ignarra, G. Karagiorgi, M. Shaevitz, and J. Spitz, *Sterile Neutrino Fits to Short Baseline Neutrino Oscillation Measurements*, *Adv.High Energy Phys.* **2013** (2013) 163897, [[arXiv:1207.4765](#)].
- [15] J. Kopp, P. A. N. Machado, M. Maltoni, and T. Schwetz, *Sterile Neutrino Oscillations: The Global Picture*, *JHEP* **1305** (2013) 050, [[arXiv:1303.3011](#)].
- [16] C. Giunti, M. Laveder, Y. Li, and H. Long, *Pragmatic View of Short-Baseline Neutrino Oscillations*, *Phys.Rev.* **D88** (2013) 073008, [[arXiv:1308.5288](#)].
- [17] P. Huber, M. Lindner, and W. Winter, *Simulation of long-baseline neutrino oscillation experiments with GLOBES*, *Comput. Phys. Commun.* **167** (2005) 195, [[hep-ph/0407333](#)].
- [18] P. Huber, J. Kopp, M. Lindner, M. Rolinec, and W. Winter, *New features in the simulation of neutrino oscillation experiments with GLOBES 3.0*, *Comput. Phys. Commun.* **177** (2007) 432–438, [[hep-ph/0701187](#)].
- [19] W. Grimus and T. Schwetz, *Four neutrino mass schemes and the likelihood of (3+1) mass spectra*, *Eur.Phys.J.* **C20** (2001) 1–11, [[hep-ph/0102252](#)].
- [20] S. Palomares-Ruiz, S. Pascoli, and T. Schwetz, *Explaining LSND by a decaying sterile neutrino*, *JHEP* **0509** (2005) 048, [[hep-ph/0505216](#)].
- [21] M. Maltoni and T. Schwetz, *Sterile neutrino oscillations after first MiniBooNE results*, *Phys. Rev.* **D76** (2007) 093005, [[arXiv:0705.0107](#)].
- [22] T. Schwetz, M. Tortola, and J. Valle, *Global neutrino data and recent reactor fluxes: status of three-flavour oscillation parameters*, *New J.Phys.* **13** (2011) 063004, [[arXiv:1103.0734](#)].
- [23] M. Gonzalez-Garcia, M. Maltoni, J. Salvado, and T. Schwetz, *Global fit to three neutrino mixing: critical look at present precision*, *JHEP* **1212** (2012) 123, [[arXiv:1209.3023](#)].
- [24] J. Kopp, M. Maltoni, and T. Schwetz, *Are there sterile neutrinos at the eV scale?*, *Phys.Rev.Lett.* **107** (2011) 091801, [[arXiv:1103.4570](#)].

- [25] C. Kraus, A. Singer, K. Valerius, and C. Weinheimer, *Limit on sterile neutrino contribution from the Mainz Neutrino Mass Experiment*, *Eur.Phys.J.* **C73** (2013) 2323, [[arXiv:1210.4194](#)].
- [26] A. Belesev et al., *An upper limit on additional neutrino mass eigenstate in 2 to 100 eV region from 'Troitsk nu-mass' data*, *JETP Lett.* **97** (2013) 67–69, [[arXiv:1211.7193](#)].
- [27] A. Atre, T. Han, S. Pascoli, and B. Zhang, *The Search for Heavy Majorana Neutrinos*, *JHEP* **0905** (2009) 030, [[arXiv:0901.3589](#)].
- [28] B. Bhattacharya, A. M. Thalapillil, and C. E. Wagner, *Implications of sterile neutrinos for medium/long-baseline neutrino experiments and the determination of  $\theta_{13}$* , *Phys.Rev.* **D85** (2012) 073004, [[arXiv:1111.4225](#)].
- [29] C. Zhang, X. Qian, and P. Vogel, *Reactor Antineutrino Anomaly with known  $\theta_{13}$* , *Phys.Rev.* **D87** (2013) 073018, [[arXiv:1303.0900](#)].
- [30] M. Maltoni and T. Schwetz, *Testing the statistical compatibility of independent data sets*, *Phys. Rev.* **D68** (2003) 033020, [[hep-ph/0304176](#)].
- [31] **Planck Collaboration** Collaboration, P. Ade et al., *Planck 2013 results. XVI. Cosmological parameters*, [arXiv:1303.5076](#).
- [32] S. Hannestad, I. Tamborra, and T. Tram, *Thermalisation of light sterile neutrinos in the early universe*, *JCAP* **1207** (2012) 025, [[arXiv:1204.5861](#)].
- [33] J. Hamann, S. Hannestad, G. G. Raffelt, and Y. Y. Wong, *Sterile neutrinos with eV masses in cosmology: How disfavoured exactly?*, *JCAP* **1109** (2011) 034, [[arXiv:1108.4136](#)].
- [34] G. Gelmini, S. Palomares-Ruiz, and S. Pascoli, *Low reheating temperature and the visible sterile neutrino*, *Phys.Rev.Lett.* **93** (2004) 081302, [[astro-ph/0403323](#)].
- [35] C. M. Ho and R. J. Scherrer, *Sterile Neutrinos and Light Dark Matter Save Each Other*, *Phys.Rev.* **D87** (2013) 065016, [[arXiv:1212.1689](#)].
- [36] G. M. Fuller, C. T. Kishimoto, and A. Kusenko, *Heavy sterile neutrinos, entropy and relativistic energy production, and the relic neutrino background*, [arXiv:1110.6479](#).
- [37] R. Foot and R. Volkas, *Reconciling sterile neutrinos with big bang nucleosynthesis*, *Phys.Rev.Lett.* **75** (1995) 4350, [[hep-ph/9508275](#)].
- [38] Y.-Z. Chu and M. Cirelli, *Sterile neutrinos, lepton asymmetries, primordial elements: How much of each?*, *Phys.Rev.* **D74** (2006) 085015, [[astro-ph/0608206](#)].
- [39] N. Saviano et al., *Multi-momentum and multi-flavour active-sterile neutrino oscillations in the early universe: role of neutrino asymmetries and effects on nucleosynthesis*, *Phys.Rev.* **D87** (2013) 073006, [[arXiv:1302.1200](#)].
- [40] L. Bento and Z. Berezhiani, *Blocking active sterile neutrino oscillations in the early universe with a Majoron field*, *Phys.Rev.* **D64** (2001) 115015, [[hep-ph/0108064](#)].
- [41] S. Hannestad, R. S. Hansen, and T. Tram, *How secret interactions can reconcile sterile neutrinos with cosmology*, [arXiv:1310.5926](#).
- [42] B. Dasgupta and J. Kopp, *A ménage à trois of eV-scale sterile neutrinos, cosmology, and structure formation*, [arXiv:1310.6337](#).
- [43] G. Karagiorgi, M. Shaevitz, and J. Conrad, *Confronting the short-baseline oscillation anomalies with a single sterile neutrino and non-standard matter effects*, [arXiv:1202.1024](#).